Physica B 405 (2010) 1980–1985

Contents lists available at ScienceDirect

Physica B

journal homepage: www.elsevier.com/locate/physb

Electronic structures of silicon doped ZnO

R. Chowdhury [a,*], P. Rees [a], S. Adhikari [a], F. Scarpa [b], S.P. Wilks [a]

[a] Swansea University, Swansea, UK
[b] University of Bristol, Bristol, UK

ARTICLE INFO

Article history:
Received 12 December 2009
Received in revised form
12 January 2010
Accepted 13 January 2010

Keywords:
Wurtzite ZnO
First-principles
Electronic structure

ABSTRACT

We have calculated the electronic structure of ZnO systems doped with Silicon (Si) using generalized gradient approximation. We found that a donor level is formed while Zn is substituted by Si. The variation in band gap is calculated as a function of Si concentration in $Zn_{1-x}Si_xO$ ($0 \le x \le 12.5$) system and comparisons are made with recently published experimental results. Further, we observed that, substitution of Si at O site forms deep acceptor levels near the top of the valence band, and thereby a weak p-type transformation of the system can be realized.

1. Introduction

ZnO is a wide-gap semiconductor [1] and a promising material for electronic, ferroelectric, piezoelectric and optical applications [2–11]. With a band gap of ~3.37 eV [12–14] and a large exciton binding energy (~60 meV) at room temperature, ZnO [15] has many potential applications in optoelectronic devices including blue and ultraviolet lasers, light-emitting diodes, and solar cells [16,2,17]. However, possible applications for ZnO [18] are currently limited due to the difficulty in achieving p-type doping of this semiconductor, which is always grown as n-type [19,20] with many donor defects, such as O vacancy (V_O) and interstitial Zn (Zn_i) [12]. Therefore, it is very difficult to dope ZnO to act as a p-type [21–23] semiconductor because of the self-compensation by the donor defects [24]. Therefore, the development and application of ZnO-based optoelectronic devices [25] has been limited due to the lack of ZnO p–n junctions [26]. There have been many attempts to obtain the p-type ZnO [27–29] by using different forms of dopant sources with group I, V, and III–V elements [30–33,21,22,34–36]. Due to the key role of Silicon (Si) in the modern semiconductor industry it is inevitable that researchers are very comfortable with working with Si for growing nanostructures. Additionally, Si is also a well known dopant that predominantly occupies cation sites in III–V semiconductors to improve their electrical and optical properties [28]. Therefore, using Si as a dopant material in ZnO might not only tune the electronic properties of ZnO but also enhance its usefulness in Si-related devices. The similarity of Si and Zn atoms in terms of their electronegativity of 1.9 and 1.65, respectively and also their comparable atomic sizes of 0.117 and 0.133 nm respectively) [37]. As a rule, Si tends to diffuse quickly into the ZnO lattice and forms a new phase Zn_2SiO_4, especially under high temperature [28].

In this paper, we calculate the electronic band structure of ZnO doped with Si using first-principles density functional theory [38–41]. We investigate two kinds of defects in ZnO, namely the substitution of Zn by Si and O by Si. The electronic band structures and density of states functions are calculated for each case. The results obtained show that when Zn is substituted by Si, the donor levels are formed. When O is substituted by Si, deep acceptor levels are formed near the top of the valence band, and, thus, a weak p-type transformation of the system can be achieved. Following the process of coexisting substitution of Zn and O by Si, the donor levels provided by the former are used to satisfy the broken bonds due to the latter, so that doping produces no free carriers of either type. This forms the self compensation is due to doping.

2. Computational approach

The ideal ZnO has a hexagonal wurtzite structure with the space group P63/mc and C6v-4 symmetry [42]. The cell parameters are $a = b = 3.249$ Å, $c = 5.206$ Å, $\alpha = \beta = 90^\circ$, and $\gamma = 120^\circ$ [42]. To illustrate the atom coordinates, a $2 \times 2 \times 2$ [12,13] supercell (with 28 atoms) of the wurtzite ZnO is shown in Fig. 1, which is frequently used in defect studies of ZnO. The O^{2-} coordination polyhedron is an O–Zn_4 tetrahedron, so it is a Zn_{2+}

* Corresponding author. Tel.: +44 1792 602088; fax: +44 1792 295676.
E-mail addresses: R.Chowdhury@swansea.ac.uk (R. Chowdhury), P.Rees@swansea.ac.uk (P. Rees), S.Adhikari@swansea.ac.uk (S. Adhikari), F.Scarpa@bristol.ac.uk (F. Scarpa), S.P.Wilks@swansea.ac.uk (S.P. Wilks).

0921-4526/$ - see front matter © 2010 Elsevier B.V. All rights reserved.
doi:10.1016/j.physb.2010.01.084

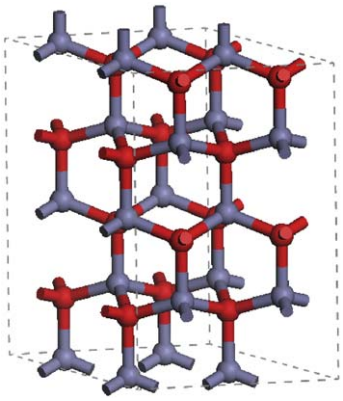

Fig. 1. Wurtzite ZnO with $2 \times 2 \times 2$ supercell. Atom colour in red corresponds to oxygen atoms and others are Zinc atoms. (For interpretation of the references to color in this figure legend, the reader is referred to the web version of this article.)

coordination polyhedron [12]. In order to address the finite size effect of the supercell, we performed the calculations considering 380 atoms (cell volume = 96 times of primitive cell) in the supercell.

The calculations are based on the density functional theory with the generalized gradient approximation (GGA) and the projector augmented wave pseudopotentials, as implemented in the CASTEP code [43,44]. The GGA with the Perdew Burke Ernzerhof exchange-correlation functional are employed in the simulations. Ultrasoft pseudopotentials [45] are utilized for the geometry optimization (BFGS algorithm) to render the computations tractable as well as to enhance efficiency. In addition we performed calculation using screened exchange functional with LDA correlation (sX-LDA) [46]. sX-LDA is developed in the context of the generalized Kohn–Sham procedure [47], which allow to split the exchange contribution to the total energy into a screened, nonlocal and a local density component. However, this is exceedingly complex and extremely time consuming. Norm-conserving pseudopotentials are used with sX-LDA functional. In our calculation, a $4 \times 4 \times 4$ kpoint MonkhorstPack mesh [48] in the Brillouin zone is used, the cutoff energy of the plane wave is 460 eV, and the calculation precision is set to be 2.0×10^{-5} eV/atom. All atoms were allowed to relax until the force on each atom was below 0.01 eV/Å and displacement of each atom was below 0.005 Å.

3. Results and discussion

First, the supercell is optimized in the calculation. The optimized results of the primitive cell of pure ZnO are presented in Table 1. The optimized geometry parameters and formation energies are in good agreement with experimental results [42] and previous theoretical prediction. Our calculated ground state properties are tabulated in Table 2, which are in good agreement with other GGA and local density approximation (LDA) results [51–53]. Table 2 lists the calculated binding energies E_b, bulk modulus B_0 and band gap in different studies. We first calculate the electronic structure of the undoped ZnO crystal using GGA and sX-LDA functionals. Kohn–Sham schemes based on GGA functionals have a common feature: it underestimate the band gap substantially and in the present case it is about 0.73 eV, which is in good agreement with other the calculations [55,12,56,49] but significantly smaller than the experimental value 3.37 eV [54,42]. This does not affect the accuracy of the description of the total energy and related properties of crystals and molecules (equilibrium structure, vibrational spectra, elastic

Table 1
Comparison of the optimized results of the primitive cell of ZnO and the experimental data.

	a (Å)	c (Å)	c/a	V_0 (Å^3)	ΔH_f
Computed value (GGA functional)	3.2832	5.2983	1.6137	49.461	−3.06
Computed value (sX-LDA functional)	3.2493	5.2054	1.6020	47.595	−3.6
HSE approach [49]	3.2300	5.2500	1.6253	–	−3.66
Experimental value [42,12,50]	3.2501	5.2071	1.6021	48.335	−3.64

Table 2
Comparison of the present work and other calculations and the experimental data.

	E_b (eV)	B_0 (GPa)	Band gap (eV)
Present work	7.46	138	0.73
GGA-PW91 [51]	7.35	136	0.91
GGA [52,53]	7.69	149	0.75
LDA [53]	9.769	162.3	0.79
Experiment [54,42]	7.56	142.6	3.37

constants, etc.). However, an accurate description of the details of the electronic structure is often required to understand the properties of semiconductors and insulators. The DFT band gap error can be corrected either by using hybrid functional (sX-LDA functional used in this study) or introducing an empirical scissors correction. Using sX-LDA functional we found that band gap error is −0.59%, compared with experiment. But this approach is extremely time consuming and it would be much suitable for crystal structure with primitive cell. For semiconductors, it is shown computationally (by comparing GW approximation and DFT band structures) that most of the difference between Kohn–Sham eigenvalues and the true excitation energies can be accounted for by a rigid shift of the conduction band upward with respect to the valence band [57]. This is attributed to a discontinuity in the exchange-correlation potential as the system goes from (N)-electrons to (N+1)-electrons during the excitation process. Using the same approach, named as scissor approximation (SA), we found that calculated the band gap becomes 3.37 eV, which is in excellent agreement with the experimental results as well with sX-LDA functional result. However, for the doped system only GGA functional used to enhance computational efficiency.

The electronic band structure and density of states (DOS) are shown in Fig. 2. It is evident that the bottom of the conduction band and the top of the valence band are at the same k-point (Γ) in the Brillouin zone confirming that ZnO is a typical direct band gap semiconductor. In the DOS and partial DOS (PDOS) (ref. Fig. 2(b)) of the undoped ZnO, the valance band can be divided into two regions: the upper valence band within −3.85 to −0.08 eV and the lower valence band within −6.32 to −3.85 eV which extends to −18.28 eV. The valence band edges near the Fermi energy for O atom are quite sharp (ref. Fig. 2(b)iii), while the conduction band edges near the Fermi energy are not. The valance band, which lies between Fermi level to −3.85 eV, is composed of the O 2p orbital states with a small contribution from Zn (3d) states. The lower valance is mainly formed by 2p state of O and 3d states of Zn.

We now consider the case that one Zn atom is replaced by one Si atom in the supercell. The band structure and DOS of the doped system are shown in Fig. 3. Compared with pure ZnO, the conduction band still minimum at the Γ- point, while the valence band maximum is shifted from the Γ- point to the F-point. The

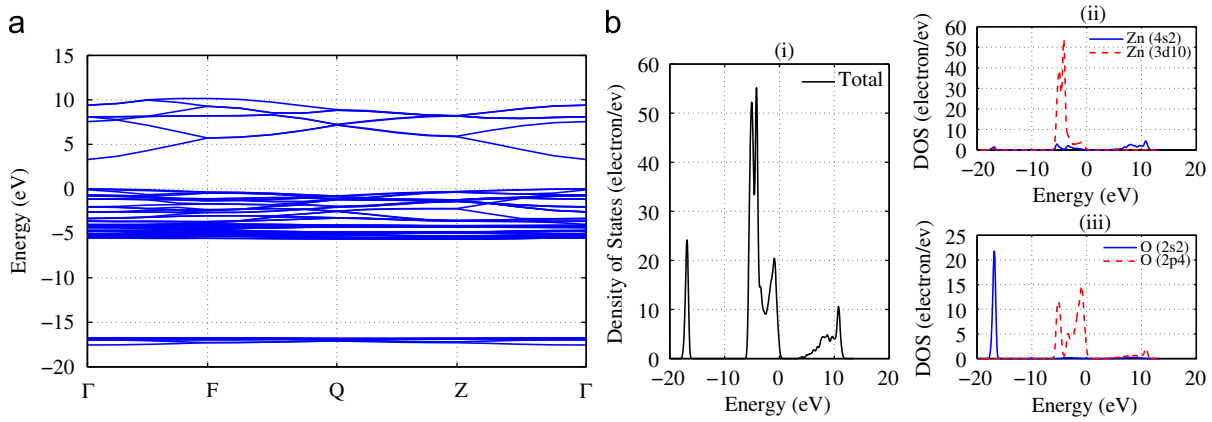

Fig. 2. Electronic band structure and of density of states of pure ZnO crystal. (a) It is evident that ZnO is a typical direct band gap semiconductor, which corresponds to a band gap is about 0.73 eV using GGA functional; 3.37 eV functional using SA approach with GGA and 3.39 eV using sX-LDA functional. The valance band can be divided into two regions: the upper valence band within −3.85 to −0.08 eV and the lower valence band within −6.32 to −3.85 eV which extends to −18.28 eV. (b) (i) Total DOS, (ii) contribution of Zn from each energy band to a given atomic orbital 3d and 4s, (ii) partial DOS contributed by O with 2p and 2s states. The valence band edges near the Fermi energy for O atom are quite sharp, while the conduction band edges near the Fermi level are not. The valance band, which lies between Fermi level to −3.85 eV, is composed of the O 2p orbital states with a small contribution from Zn (3d) states. The lower valance is mainly formed by 2p state of O and 3d states of Zn.

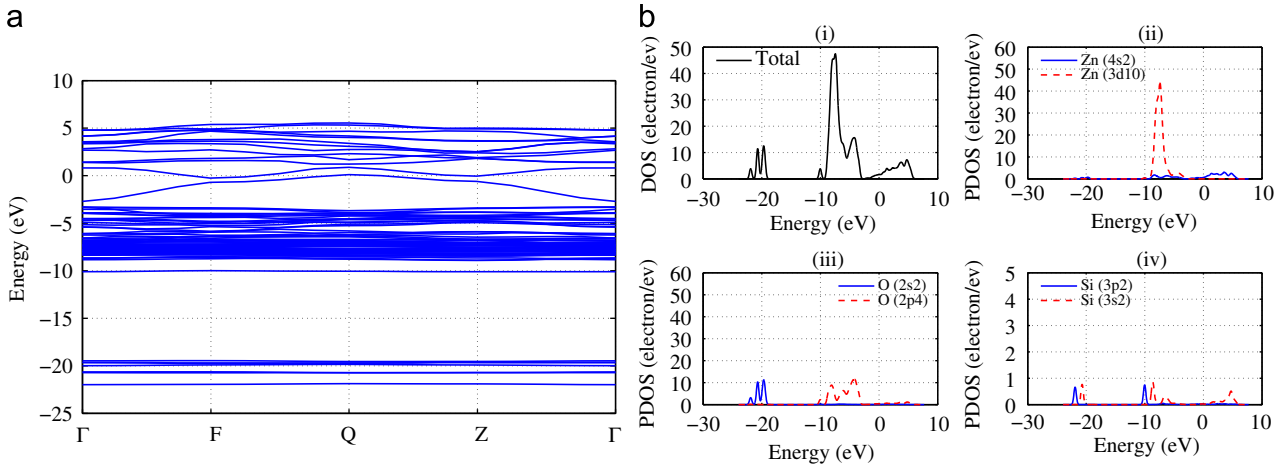

Fig. 3. Electronic band structure and of density of states of doped ZnO crystal with Si_{Zn} without adopting SA approach for correcting band gap error. (a) Dopant reduces the band gap from 0.73 to 0.63 eV using GGA functional. A new occupied band, is recognized near to −10 eV of the valence band of Si_{Zn}. This can therefore be regarded as a defect state induced by Si_{Zn}. (b) (i) Total DOS, (ii) partial DOS contributed Zn with 3d and 4s, (iii) partial DOS contributed by O with 2p and 2s states, and (iv) DOS contributed by doped Si at Zn site. Compared to pure ZnO crystal, the valence band edges near the Fermi energy for O atom are not sharp here. The valance band, which lies near to −10 eV, is composed of the O 2p orbital states and small contribution from 3p state of Si. The upper valance band is mainly formed by 3d state of Zn and the O 2p orbital states.

observed band gap reduces significantly. The narrowing of band gap observed in the present study supported by other studies [28,58]. Zinc atom contributes two valence electrons, while Si contributes four valence electrons. Therefore, fixed positive charge is placed at Si occupied Zn lattice site along with two additional electrons. This makes the doped ZnO model with donor impurities. Since the binding energy is measured relative to the energy of the conduction band levels from which impurity level is formed, it can be understood that donor impurity introduces additional electron levels at the bottom of the conduction band. So, Si_{Zn} is formed as n-type semiconductor. According to a recent study on Si doped ZnO films [29], Si actually exists in four different oxidation states, namely, Si^{+4}, Si^{+3}, Si^{+2}, Si^{+1} [59]. To see the determine the effect of these different oxidation states we applied the DFT calculation, however, we did not observe any effect on the band gap narrowing [60] due to these different oxidation states of Si. Limited research exists on band gap narrowing of ZnO by impurity incorporation [58]. In this study, we continued to the study effect of different concentration of Si on $Zn_{1-x}Si_xO$ system. It is found that (ref. Fig. 4), for one Si, i.e., $x=0.0625$, we found a total reduction in band gap, $\Delta E_g = E_g(\text{ZnO}) - E_g(\text{Si–ZnO})$, is about 0.22 eV compared to undoped system. The results is similar to the theoretical work by Ferhat et al. [58] for Cu doped ZnO. The origin of the reduction in the band gap of the Si-doped ZnO can be anticipated due to the hybridization of the Si 3s bands with the O 2p bands. We also performed our calculation incorporating Burstein–Moss (BM) shift [61,29] and band gap narrowing (BGN) developed for heavily doped semiconductors [29,62,63].To calculate the BM shift (ΔE_{BM}) and the resulting band gap (E_{BM}), we used the standard expression, given in [29] as

$$E_{BM} = E_0 + \Delta E_{BM} \tag{1}$$

where

$$\Delta E_{BM} = \frac{\hbar^2}{8\pi^2}(3\pi^2 n)^{2/3}\left(\frac{1}{m_e^*} + \frac{1}{m_h^*}\right) \tag{2}$$

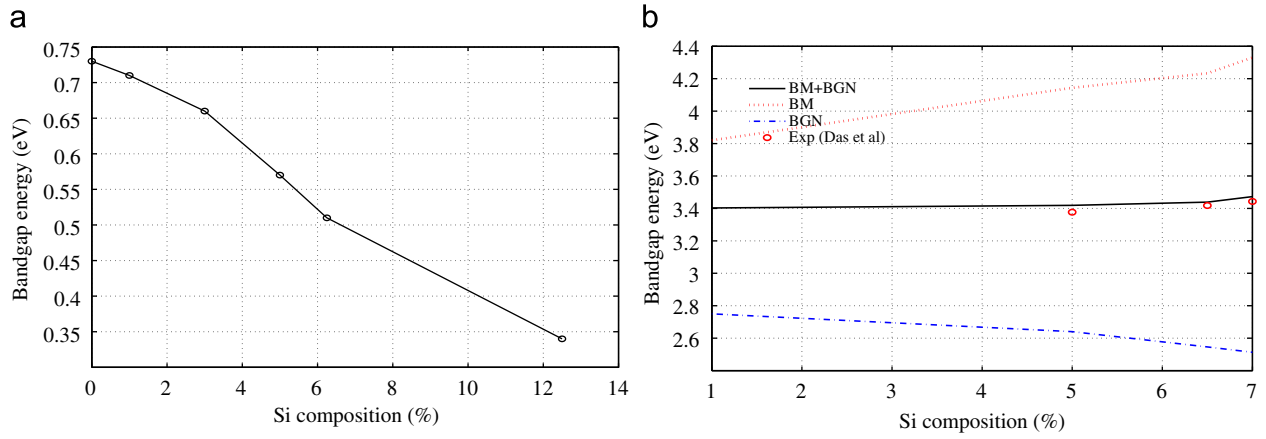

Fig. 4. (a) Effect of Si on ZnO crystal. Dopant reduces the band gap from 0.73 to 0.34 eV at 12.5% Si composition using GGA functional. Total reduction in band gap, $\Delta E_g = E_g(\mathrm{ZnO}) - E_g$ (Si–ZnO), is about 0.39 eV compared to undoped system. (b) Open circles are the experimental data points from [29]. Line corresponds to BM is the band gap calculation considering only BM shift effect. Line corresponds to BGN is the band gap calculation considering only band gap narrowing effect. Line corresponds to BM+BGN is the band gap calculation considering both BM shift and band gap narrowing effect.

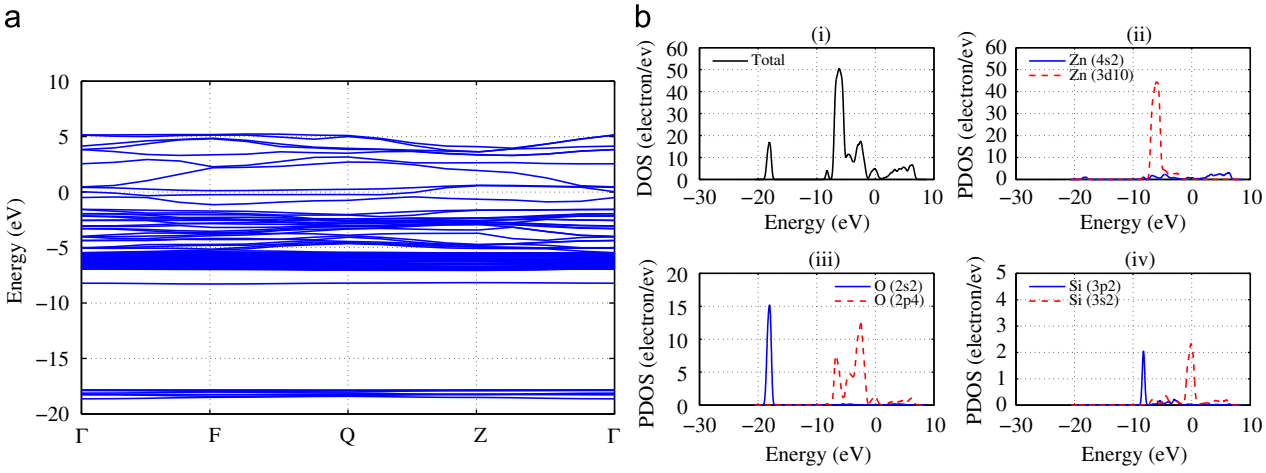

Fig. 5. Electronic band structure and of density of states of doped ZnO crystal with Si_O without adopting SA approach for correcting band gap error. (a) A new occupied band, is recognized near to −8 eV of the valence band of Si_O. This can therefore be regarded as a defect state induced by Si_O. (b) (i) Total DOS, (ii) partial DOS contributed Zn with 3d and 4s, (iii) partial DOS contributed by O with 2p and 2s states, and (iv) DOS contributed by doped by Si occupied O lattice site. The hybridization between Si (3s) states and Zn (3d) states which are near the top of the valence band leads to the acceptor level. The valence band edges at the Fermi level for Si atom with 3s state are quite sharp, while the contribution from either Zn or O near the Fermi level are not. The lower valance near to −20 eV is mainly formed by 2s state of O.

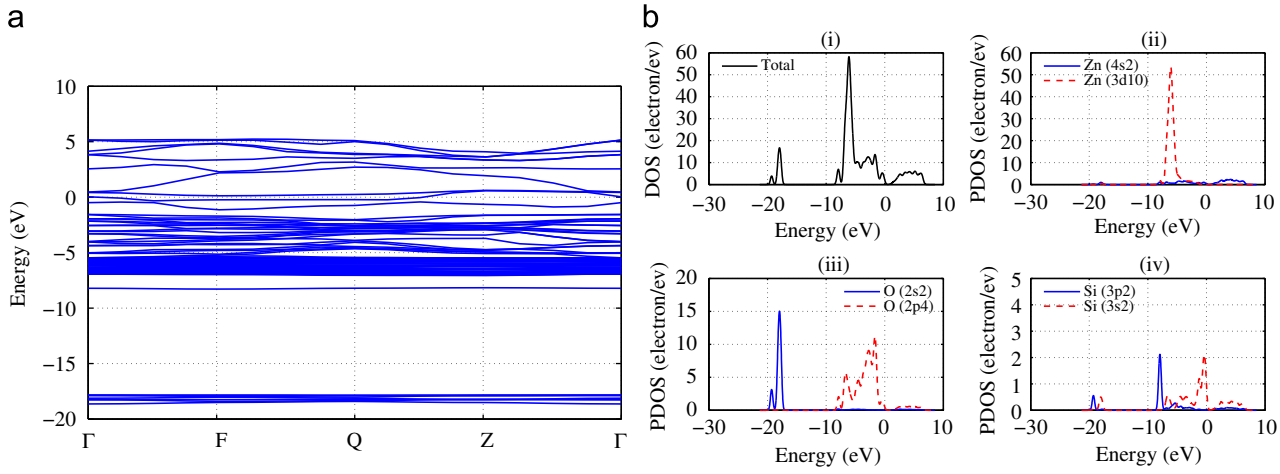

Fig. 6. Electronic band structure and of density of states of doped ZnO crystal coexisting substitution of Zn and O by Si without adopting SA approach for correcting band gap error. (a) Doped ZnO with Si_{Zn} and Si_O makes the crystal as self compensated system. (b) (i) Total DOS, (ii) partial DOS contributed Zn with 3 and 4 (iii) partial DOS contributed by O with 2p and 2s states, and (iv) DOS contributed by doped Si at Zn and O sites. The valence band edges at the Fermi level for Si atom with 3s state are quite sharp, while the contribution from either Zn or O near the Fermi level are not. The lower valance near to −20 eV is mainly formed by 2s state of O.

In Eq. (1), E_0 is the band gap of undoped ZnO and taken from GGA functional with SA. In Eq. (2), n is the density of electrons at different Si concentrations, m_e^* is the effective mass of electrons taken as $0.28m_e$ and m_h^* is the effective mass of the holes taken as $0.59m_e$ and m_e represents the free electron mass [29]. $\hbar$ and π are the usual constants. Variation in the band gap of ZnO with increasing Si concentration, calculated from the above formula of the BM shift is shown in Fig. 4(b) by the dotted line. The experimental values of the band gap are presented by the open circle in the same figure. It can be observed that, the band gap obtained from the BM shift alone is higher than that observed for the experimental values. Therefore, the BM shift alone cannot explain the observed band gap variation with the impurity concentration. For incorporation of band gap narrowing, we used similar formalism used in [29,60] as

$$E_{BGN} = E_0 - \Delta E_{BGN} \tag{3}$$

where

$$\Delta E_{BGN} = \Delta E_{ex} + \Delta E_{eh} + \Delta E_{ei} + \Delta E_{hi} \tag{4}$$

In the above equations ΔE_{ex} is the energy due to exchange interaction amongst electron that causes shift of the conduction band edge; ΔE_{eh} is the energy due to electron-hole interaction; ΔE_{ei} is the energy due to electron-impurity interaction and ΔE_{eh} is the energy due to impurity hole interaction. The total band gap, considering both the BM shift and the band gap narrowing, can be expressed following [29] as

$$E_{BM+BGN} = E_0 + \Delta E_{BM} - \Delta E_{BGN} \tag{5}$$

It can be observed that, the band gap obtained from the band gap narrowing alone is lower than that observed experimental values. However, combined effect of BM shift and band gap narrowing predicts reasonably accurate band gap variation as observed in experiment.

Next, we consider the case that one O atom is substituted by one Si atom in the supercell. The band and DOS of the doped system are shown in Fig. 5. A new narrow band exists nearby -8 eV, which is contributed by Si 3 p states. In addition, the DOS near the Fermi level increases because of the contribution by Si 3 p states. Oxygen atom contributes six valence electrons, while Si contributes four valence electrons. Therefore, fixed charge is placed at Si occupied O lattice site along with presence of two less electrons in the crystal. This makes the doped ZnO model with acceptor impurities. The missing electrons can be treated as a bound hole with a binding energy that is small on the scale of energy band. In terms of band picture, this hole is manifested as an additional electronic level (at about 0.39 eV) lying slightly above the top of valence band. The binding energy of the hole excites electrons from the top of the valence band into acceptor level. This suggests that, that Si_O is expected to induce a deep acceptor level [13,2,27]. Thus, a weak p-type transformation can be realized by Si_O. The result is in accord with the report [64] which suggested that it is 0.4 eV above the valence band maximum. Similar observations are found for altering the doping sites.

Finally, we consider the case that one Zn atom and one O atom are simultaneously substituted by Si atoms in the supercell, and the substituted Zn atom and O atom are adjacent. The band and the DOS of the doped system are shown in Fig. 6. Compared with pure ZnO, the conduction band is still minimum at the Γ- point, while the valence band maxima is shifted from the F-point to the Γ- point. Following the process of coexisting substitution of Zn and O by Si, the extra core electrons provided by the former are used to satisfy the broken bonds due to the latter, so that doping produces no free carriers of either type. This forms the self compensation due to doping.

4. Conclusion

We have performed first-principles calculations of Si-doped ZnO systems with Si at different sites. The obtained results show that when Zn is substituted by Si donor levels are formed. When Oxygen is substituted by Si, the system deep acceptor levels are formed near the top of the valence band, and, thus, a weak p-type transformation of the system is achieved. When the two kinds of substitutes coexist, the donor level contributed by Si_{Zn} is compensated by Si_O, which makes difficult for p-type transformation. Excellent agreements have been achieved with experimental results, while considering bandgap narrowing and BM shift effect.

Acknowledgements

RC acknowledges the support of Royal Society through the award of Newton International Fellowship. SA gratefully acknowledges the support The Leverhulme Trust for the award of the Philip Leverhulme Prize.

References

[1] U. Ozgur, Y. Alivov, C. Liu, A. Teke, M. Reshchikov, S. Dogan, V. Avrutin, S. Cho, H. Morkoc, Journal of Applied Physics 98 (2005).
[2] D. Look, D. Reynolds, J. Sizelove, R. Jones, C. Litton, G. Cantwell, W. Harsch, Solid State Communications 105 (1998) 399.
[3] R. Khanna, K. Ip, Y. Heo, D. Norton, S. Pearton, F. Ren, Applied Physics Letters 85 (2004) 3468.
[4] A. Polyakov, N. Smirnov, A. Govorkov, E. Kozhuichova, S. Pearton, D. Norton, A. Osinsky, A. Dabiran, Journal of Electronic Materials 35 (2006) 663.
[5] L. Xin-Hua, X. Jia-Yue, J. Min, S. Hui, L. Xiao-Min, Chinese Physics Letters 23 (2006) 3356.
[6] H. Pan, J.B. Yi, L. Shen, R.Q. Wu, J.H. Yang, J.Y. Lin, Y.P. Feng, J. Ding, L.H. Van, J.H. Yin, Physical Review Letters 99 (2007).
[7] X. Wang, X. Chen, R. Dong, Y. Huang, W. Lu, Physics Letters A 373 (2009) 3091.
[8] T.S. Herng, S.P. Lau, L. Wang, B.C. Zhao, S.F. Yu, M. Tanemura, A. Akaike, K.S. Teng, Applied Physics Letters 95 (2009).
[9] Z. Fu-Chun, Z. Zhi-Yong, Z. Wei-Hu, Y. Jun-Feng, Y. Jiang-Ni, Chinese Physics Letters 26 (2009).
[10] Y. Xing, Z. Xi, Z. Xue, X. Zhang, J. Song, R. Wang, J. Xu, Y. Song, S. Zhang, D. Yu, Applied Physics Letters 83 (2003) 1689.
[11] K. Xuan, X. Yan, S. Ding, Y. Yang, Y. Xiao, Z. Guo, Chinese Physics 15 (2006) 460.
[12] S. Panpan, S. Xiyu, H. Qinying, L. Yadong, C. Wei, Journal of Semiconductors 30 (2009).
[13] Q. Wan, Z. Xiong, J. Dai, J. Rao, F. Jiang, Optical Materials 30 (2008) 817821.
[14] Y. Yu-Rong, Y. Xiao-Hong, G. Zhao-Hui, D. Yu-Xiang, Chinese Physics B 17 (2008) 3433.
[15] F. Decremps, F. Datchi, A. Saitta, A. Polian, S. Pascarelli, A. Di Cicco, J. Itie, F. Baudelet, Physical Review B 68 (2003).
[16] Z. Tang, G. Wong, P. Yu, M. Kawasaki, A. Ohtomo, H. Koinuma, Y. Segawa, Applied Physics Letters 72 (1998) 3270.
[17] J. Huepkes, B. Rech, O. Kluth, T. Repmann, B. Zwaygardt, J. Mueller, R. Drese, M. Wuttig, Solar Energy Materials and Solar Cells 90 (2006) 3054.
[18] X. Shen, P.B. Allen, J.T. Muckerman, J.W. Davenport, J.-C. Zheng, Nano Letters 7 (2007) 2267.
[19] T. Murphy, J. Blaszczak, K. Moazzami, W. Bowen, J. Phillips, Journal of Electronic Materials 34 (2005) 389.
[20] M.D. McCluskey, S.J. Jokela, Physica B—Condensed Matter 401 (2007) 355.
[21] Y. Ryu, S. Zhu, D. Look, J. Wrobel, H. Jeong, H. White, Journal of Crystal Growth 216 (2000) 330.
[22] M. Kumar, T.-H. Kim, S.-S. Kim, B.-T. Lee, Applied Physics Letters 89 (2006).
[23] L. Dong, Q.-Q. Sun, Y. Shi, H.-W. Guo, H. Liu, C. Wang, S.-J. Ding, D.W. Zhang, Thin Solid Films 517 (2009) 4355.
[24] C. Park, S. Zhang, S. Wei, Physical Review B 66 (2002).
[25] D. Look, B. Claftin, Physica Status Solidi B–Basic Research 241 (2004) 624.
[26] J. Bian, X. Li, C. Zhang, W. Yu, X. Gao, Applied Physics Letters 85 (2004) 4070.
[27] D. Look, D. Reynolds, C. Litton, R. Jones, D. Eason, G. Cantwell, Applied Physics Letters 81 (2002) 1830.
[28] J. Zhao, L. Qin, L. Zhang, Physica E-Low—Dimensional Systems & Nanostructures 40 (2008) 795.
[29] A.K. Das, P. Misra, L.M. Kukreja, Journal of Physics D—Applied Physics 42 (2009).
[30] K. Kim, H. Kim, D. Hwang, J. Lim, S. Park, Applied Physics Letters 83 (2003) 63.

[31] Y. Heo, S. Park, K. Ip, S. Pearton, D. Norton, Applied Physics Letters 83 (2003) 1128.
[32] K. Bang, D. Hwang, M. Park, Y. Ko, I. Yun, J. Myoung, Applied Surface Science 210 (2003) 177.
[33] T. Aoki, Y. Hatanaka, D. Look, Applied Physics Letters 76 (2000) 3257.
[34] S. Limpijumnong, X. Li, S. Wei, S. Zhang, Physica B—Condensed Matter 376 (2006) 686.
[35] X. Guo, H. Tabata, T. Kawai, Journal of Crystal Growth 223 (2001) 135.
[36] D. Look, G. Renlund, R. Burgener, J. Sizelove, Applied Physics Letters 85 (2004) 5269.
[37] X. An, G. Meng, Q. Wei, L. Zhang, Crystal Growth & Design 6 (2006) 1967.
[38] N.H. Moreira, G. Dolgonos, B. Aradi, A.L. da Rosa, T. Frauenheim, Journal of Chemical Theory and Computation 5 (2009) 605.
[39] B. Wang, S. Nagase, J. Zhao, G. Wang, Nanotechnology 18 (2007).
[40] Y.R. Yang, X.H. Yan, Y. Xiao, Z.H. Guo, Chemical Physics Letters 446 (2007) 98.
[41] N.H. Moreira, A.L. da Rosa, T. Frauenheim, Applied Physics Letters 94 (2009).
[42] E. Kisi, M. Elcombe, Acta Crystallographica Section C—Crystal Structure Communications 45 (1989) 1867.
[43] S. Clark, M. Segall, C. Pickard, P. Hasnip, M. Probert, K. Refson, M. Payne, Zeitschrift Fur Kristallographie 220 (2005) 567.
[44] M. Segall, P. Lindan, M. Probert, C. Pickard, P. Hasnip, S. Clark, M. Payne, Journal of Physics—Condensed Matter 14 (2002) 2717.
[45] D. Vanderbilt, Physical Review B 41 (1990).
[46] J. Lento, R. Nieminen, Journal of Physics—Condensed Matter 15 (2003) 4387.
[47] A. Seidl, A. Gorling, P. Vogl, J. Majewski, M. Levy, Physical Review B 53 (1996) 3764.
[48] H. Monkhorst, J. Pack, Physical Review B 13 (1976) 5188.
[49] J.L. Lyons, A. Janotti, C.G. Van de Walle, Physical Review B 80 (2009).
[50] A. Janotti, D. Segev, C.G. Van de Walle, Physical Review B 74 (2006).
[51] Z. Fu-Chun, Z. Zhi-Yong, Z. Wei-Hu, Y. Jun-Feng, Y. Jiang-Ni, Chinese Physics B 18 (2009) 2508.
[52] P. Erhart, K. Albe, A. Klein, Physical Review B 73 (2006).
[53] J. Jaffe, J. Snyder, Z. Lin, A. Hess, Physical Review B 62 (2000) 1660.
[54] S. Desgreniers, Physical Review B 58 (1998) 14102.
[55] D. Vogel, P. Kruger, J. Pollmann, Physical Review B 52 (1995) 14316.
[56] Y. Xu, W. Ching, Physical Review B 48 (1993) 4335.
[57] R.W. Godby, Topics in Applied Physics 69 (1992).
[58] M. Ferhat, A. Zaoui, R. Ahuja, Applied Physics Letters 94 (2009).
[59] Q.-B. Ma, Z.-Z. Ye, H.-P. He, S.-H. Hu, J.-R. Wang, L.-P. Zhu, Y.-Z. Zhang, B.-H. Zhao, Journal of Crystal Growth 304 (2007) 64.
[60] S. Jain, J. Mcgregor, D. Roulston, Journal of Applied Physics 68 (1990) 3747.
[61] E. Burstein, Physical Review Letters 93 (1954) 632.
[62] G. Mahan, Journal of Applied Physics 51 (1980) 2634.
[63] J. Serre, A. Ghazali, Physical Review B 28 (1983) 4704.
[64] Y. Yan, M.M. Al-Jassim, S.-H. Wei, Applied Physics Letters 89 (2006).